Concerns about phytoplankton bloom trends in global lakes

Article *in* Nature · February 2021

DOI: 10.1038/s41586-021-03254-3

CITATIONS
4

READS
688

6 authors, including:

Lian Feng
Southern University of Science and Technology
112 PUBLICATIONS **3,181** CITATIONS
SEE PROFILE

Yanhui Dai
Southern University of Science and Technology
4 PUBLICATIONS **39** CITATIONS
SEE PROFILE

Xuejiao Hou
Wuhan University
18 PUBLICATIONS **336** CITATIONS
SEE PROFILE

Junguo Liu
Beijing Forestry University
276 PUBLICATIONS **11,055** CITATIONS
SEE PROFILE

Concerns about phytoplankton bloom trends in global lakes

https://doi.org/10.1038/s41586-021-03254-3

Received: 3 November 2019

Accepted: 10 December 2020

Published online: 17 February 2021

Check for updates

Lian Feng[1,2]✉, Yanhui Dai[1,2], Xuejiao Hou[1,2], Yang Xu[1,2], Junguo Liu[1,2] & Chunmiao Zheng[1,2]

ARISING FROM Ho, J. C. et al., *Nature* https://www.nature.com/articles/s41586-019-1648-7 (2019)

Satellite remote sensing has been widely used to monitor the water quality of inland and coastal environments. Using satellite data from the Landsat 5 Thematic Mapper (L5TM), Ho et al.[1] showed an increase in peak summertime bloom intensity in 68% of the 71 large lakes worldwide from 1982 to 2012. However, we question the veracity of their finding for at least two reasons: (1) satellite-derived reflectance in a single near-infrared (NIR) band is not a reliable proxy for bloom strength, and (2) the infrequent satellite observations from L5TM make it difficult to draw statistically meaningful conclusions.

Ho et al.[1] argued that the L5TM-estimated bloom intensity (B_{NIR}) (see equation 2 in Ho et al.[1]), which is basically the reflectance in the NIR band, represents near-surface phytoplankton biomass. However, this argument became questionable when examining the spectral and chlorophyll *a* (Chl*a*; a key indicator for phytoplankton biomass[2]) datasets collected from 15 lakes in China[3] with varying eutrophic status (Chl*a* ranging between 1.5 and 222.6 mg m^{-3}; see Extended Data Fig. 1 and Supplementary Information). The complex relationship between spectral reflectance and Chl*a* concentrations were also demonstrated by Spyrakos et al.[4] using in situ data from around the world. Theoretically, the signal in the NIR band can be attributed to various water constituents in addition to algal blooms, and the contributions from suspended sediments and the presence of aquatic plants could be two of the most common perturbations in inland lakes. Ho et al.[1] attempted to mask out sediment-rich waters with the use of hue but, as detailed later, our analysis suggests that the hue defined in ref. [1] does not accurately represent the colour of a water body.

Bloom strength tends to be substantially overestimated in sediment-rich waters. Examples from two of the lakes studied in Ho et al.[1] (Fig. 1) show that the B_{NIR} value of the high-turbidity, low-algae pixels was higher than that of the algae-present pixels within the same images. The examination of historical images (through both true-colour images and spectral features) shows that L5TM observations have captured sediment plumes in at least 58 (82%) of the 71 studied lakes, and these plumes could be incorrectly labelled as algal blooms owing to their high B_{NIR} (see Extended Data Fig. 2). As supported by previous studies using data from both of the lakes studied in Ho et al.[1] and from other global coastal/inland waters, the NIR reflectance in turbid waters can be substantially enhanced (see Extended Data Table 1). In inland lakes, episodic meteorological (for example, wind and precipitation) and hydrological (for example, riverine discharge) events can strongly influence sediment concentrations[5], as exemplified by previous studies in Lake Erie[6] and Lake Okeechobee[7] in the USA and Hongze Lake[8] in China (three lakes examined in ref. [1]). Therefore, the effect of water turbidity on B_{NIR} should be evaluated carefully.

Similar to high sediment loads, the growth of aquatic vegetation can lead to overestimation of bloom severity. Pixels with high B_{NIR}—in particular, vegetated waters rather than bloom areas—were also found within the same lakes (see Fig. 1a, b), where massive submerged plants have previously been reported[9]. The reason is that algal blooms and submerged vegetation share similarly high NIR reflectance (see Extended Data Fig. 3). Moreover, previous studies with datasets collected across various global regions and plant species also showed markedly increased NIR reflectance due to the presence of submerged vegetation (see Extended Data Table 2). Indeed, a literature search revealed that of the 71 studied lakes, 41 (58%) contain abundant aquatic plants (see Extended Data Table 3) and their effects on B_{NIR} should have been considered.

A hue-based mask (equations 3 and 4 in Ho et al.[1]) was designed to exclude potential contamination from sediments. However, this approach has failed in numerous cases (see Extended Data Fig. 2). This is mainly due to the inclusion of the atmospheric signals in the calculation of hue, that is, the hue was estimated using the top-of-atmosphere reflectance. Thus, this hue represents the colour of the combined signal of the atmosphere and the water. As shown in Extended Data Fig. 4, atmospheric molecular scattering alone could dominate the top-of-atmosphere reflectance for water bodies in the blue band[10]. The method (Fmask)[11] used to determine lake surface area could lead to substantial underestimations of bloom severity. As the examples in Fig. 1c–e and Extended Data Fig. 5 show, severe bloom areas failed to pass the Fmask and were excluded in further B_{NIR} calculations. Indeed, examination of the lakes studied in ref. [1] showed that most of the bloom scums were missed owing to the improper use of Fmask. This is because intense blooms often cause high normalized difference vegetation index (NDVI) values that can exceed the threshold used by Fmask (for example, NDVI < 0.1) to identify water pixels[11].

Furthermore, the interannual dynamics of lacustrine algal blooms are difficult to characterize by infrequent L5TM observations[12], and cloud coverage poses further challenges associated with optical satellite remote sensing. Statistically, the global mean daily cloud-free probability is 33%, with seasonal differences of <5% (ref. [13]). In other words, when L5TM overpasses 23 times in a year because of its 16-day revisit period, the annual mean number of cloud-free observations for a given location is only ~7.5 even without any other unfavourable observational conditions (such as sun glint). As a compromise between data availability and result fidelity, Ho et al.[1] excluded those years with fewer than three valid images in five summer months. We replotted a time series of algal bloom areas in Taihu Lake that was produced by Hu et al.[12] (see Extended Data Fig. 6), which was obtained using daily observations from the Moderate-resolution Imaging Spectroradiometer (MODIS) satellite (revisit period of about one image per day) between 2000 and 2008. Of the >300 cloud-free daily MODIS images within the nine-year period,

[1]School of Environmental Science and Engineering, Southern University of Science and Technology, Shenzhen, China. [2]State Environmental Key Laboratory of Integrated Surface Water-Groundwater Pollution Control, Southern University of Science and Technology, Shenzhen, China. ✉e-mail: fengl@sustech.edu.cn

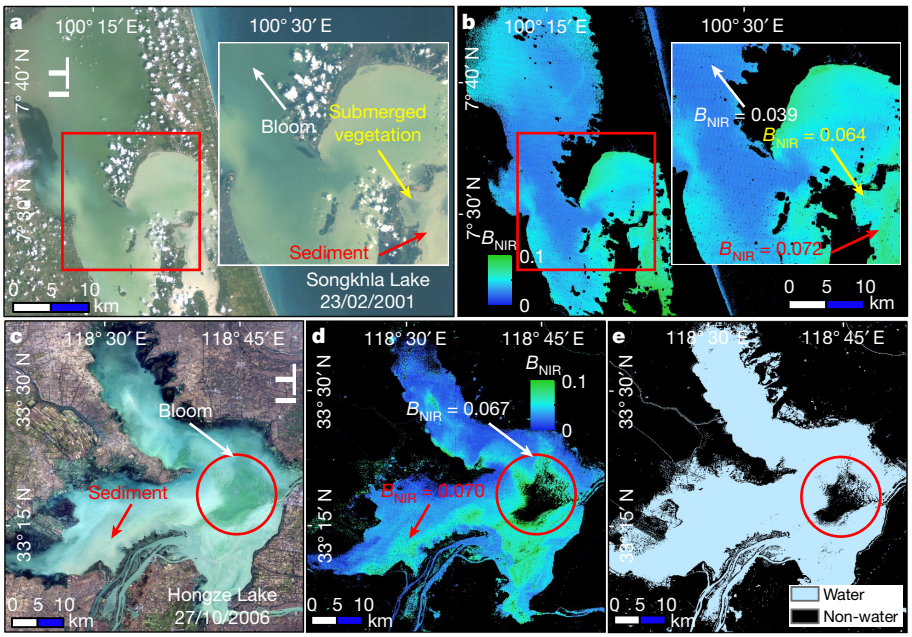

Fig. 1 | Examples showing the problems associated with L5TM-based bloom intensity (B_{NIR}) estimated with equation 2 in Ho et al.[1]. **a**–**d**, L5TM true-colour composites and corresponding B_{NIR} map for Songkhla Lake in Thailand (**a**, **b**) and Hongze Lake in China (**c**, **d**). **e**, Water mask determined by Fmask[11] for Hongze Lake using the same image as in **c**. Areas with either high sediment loads (yellowish in the true-colour images, indicated by red arrows) or the presence of submerged vegetation (dark in the true-colour images, indicated by yellow arrows) exhibit higher B_{NIR} values than the bloom-occurring pixels (greenish in the true-colour images, indicated by white arrows). An intense bloom in Hongze Lake (within the red circle) was erroneously classified as non-water by Fmask and excluded in the B_{NIR} map (**d**). The red squares in **a**, **b** indicate the inset location. More examples of these problems are shown in Extended Data Figs. 2, 5.

only 24 shared the same overpassing dates as L5TM. Furthermore, detecting a bloom on the basis of remote-sensing imagery depends strongly on wind, given that the fraction of the satellite-observable surface bloom in relation to the total phytoplankton biomass is also a function of wind speed[14,15]. Owing to the unpredictable nature of cloud occurrence and wind speed, the temporal dynamics of bloom features were difficult to characterize with L5TM datasets.

Our results suggest that the use of L5TM-based B_{NIR} by Ho et al.[1] as a proxy for algal bloom strength is questionable for the majority of the lakes examined in their study. The incorrect use of a water mask algorithm (that is, Fmask) also leads to the omission of the most severe blooms with floating scum. The use of limited Landsat observations (often one cloud-free image every 1–2 months) is problematic for drawing statistically meaningful conclusions. Therefore, the trends in phytoplankton blooms for the 71 global lakes derived by Ho et al.[1] appear unrealistic.

Reporting summary

Further information on research design is available in the Nature Research Reporting Summary linked to this paper.

Data availability

The Landsat data can be obtained from the US Geological Survey at https://glovis.usg.gov. The in situ spectral and Chl*α* data used in this paper are available in the Supplementary Information.

1. Ho, J. C., Michalak, A. M. & Pahlevan, N. Widespread global increase in intense lake phytoplankton blooms since the 1980s. *Nature* **574**, 667–670 (2019).
2. Boyce, D. G., Lewis, M. R. & Worm, B. Global phytoplankton decline over the past century. *Nature* **466**, 591–596 (2010).
3. Guan, Q. et al. Eutrophication changes in fifty large lakes on the Yangtze Plain of China derived from MERIS and OLCI observations. *Remote Sens. Environ.* **246**, 111890 (2020).
4. Spyrakos, E. et al. Optical types of inland and coastal waters. *Limnol. Oceanogr.* **63**, 846–870 (2018).
5. Bloesch, J. Mechanisms, measurement and importance of sediment resuspension in lakes. *Mar. Freshw. Res.* **46**, 295–304 (1995).
6. Valipour, R., Boegman, L., Bouffard, D. & Rao, Y. R. Sediment resuspension mechanisms and their contributions to high-turbidity events in a large lake. *Limnol. Oceanogr.* **62**, 1045–1065 (2017).
7. Wang, M., Nim, C. J., Son, S. & Shi, W. Characterization of turbidity in Florida's Lake Okeechobee and Caloosahatchee and St. Lucie estuaries using MODIS-Aqua measurements. *Water Res.* **46**, 5410–5422 (2012).
8. Cao, Z., Duan, H., Feng, L., Ma, R. & Xue, K. Climate-and human-induced changes in suspended particulate matter over Lake Hongze on short and long timescales. *Remote Sens. Environ.* **192**, 98–113 (2017).
9. Sompongchaiyakul, P., Laongsiriwong, N. & Sangkarnjanawanich, P. An occurrence of eutrophication in Songkhla Lake: a review. In *Proceedings of the International Workshop on Integrated Lake Management, Hai-Yai, Songkhla*, 19–21 (2004).
10. Gordon, H. R. Atmospheric correction of ocean color imagery in the Earth Observing System era. *J. Geophys. Res.* **102**, 17081–17106 (1997).
11. Zhu, Z., Wang, S. & Woodcock, C. E. Improvement and expansion of the Fmask algorithm: cloud, cloud shadow, and snow detection for Landsats 4–7, 8, and Sentinel 2 images. *Remote Sens. Environ.* **159**, 269–277 (2015).
12. Hu, C. et al. Moderate Resolution Imaging Spectroradiometer (MODIS) observations of cyanobacteria blooms in Taihu Lake, China. *J. Geophys. Res. Oceans* **115**, C04002 (2010).
13. King, M. D., Platnick, S., Menzel, W. P., Ackerman, S. A. & Hubanks, P. A. Spatial and temporal distribution of clouds observed by MODIS onboard the Terra and Aqua satellites. *IEEE Trans. Geosci. Remote Sens.* **51**, 3826–3852 (2013).
14. Qi, L., Hu, C., Visser, P. M. & Ma, R. Diurnal changes of cyanobacteria blooms in Taihu Lake as derived from GOCI observations. *Limnol. Oceanogr.* **63**, 1711–1726 (2018).
15. Bosse, K. R. et al. Spatial-temporal variability of in situ cyanobacteria vertical structure in Western Lake Erie: implications for remote sensing observations. *J. Great Lakes Res.* **45**, 480–489 (2019).
16. Büttner, G., Korándi, M., Gyömörei, A., Köte, Z. & Szabó, G. Satellite remote sensing of inland waters: Lake Balaton and reservoir Kisköre. *Acta Astronaut.* **15**, 305–311 (1987).
17. Bukata, R., Jerome, J. & Bruton, J. Particulate concentrations in Lake St. Clair as recorded by a shipborne multispectral optical monitoring system. *Remote Sens. Environ.* **25**, 201–229 (1988).
18. Nas, B., Ekercin, S., Karabörk, H., Berktay, A. & Mulla, D. An application of Landsat-5TM image data for water quality mapping in Lake Beysehir, Turkey. *Wat. Air Soil Pollut.* **212**, 183–197 (2010).
19. Binding, C., Jerome, J., Bukata, R. & Booty, W. Suspended particulate matter in Lake Erie derived from MODIS aquatic colour imagery. *Int. J. Remote Sens.* **31**, 5239–5255 (2010).
20. Matthews, M. W., Bernard, S. & Winter, K. Remote sensing of cyanobacteria-dominant algal blooms and water quality parameters in Zeekoevlei, a small hypertrophic lake, using MERIS. *Remote Sens. Environ.* **114**, 2070–2087 (2010).

21. Kaba, E., Philpot, W. & Steenhuis, T. Evaluating suitability of MODIS-Terra images for reproducing historic sediment concentrations in water bodies: Lake Tana, Ethiopia. *Int. J. Appl. Earth Obs. Geoinf.* **26**, 286–297 (2014).
22. Hamed, M. A. Estimation of water quality parameters in Lake Nasser using remote sensing techniques. In *Twentieth International Water Technology Conference, IWTC20* (2017).
23. Zeng, C. & Binding, C. The effect of mineral sediments on satellite chlorophyll-a retrievals from line-height algorithms using red and near-infrared bands. *Remote Sens.* **11**, 2306 (2019).
24. Mikkelsen, O. A. Variation in the projected surface area of suspended particles: Implications for remote sensing assessment of TSM. *Remote Sens. Environ.* **79**, 23–29 (2002).
25. Dekker, A., Vos, R. & Peters, S. Comparison of remote sensing data, model results and in situ data for total suspended matter (TSM) in the southern Frisian lakes. *Sci. Total Environ.* **268**, 197–214 (2001).
26. Doxaran, D., Froidefond, J.-M., Lavender, S. & Castaing, P. Spectral signature of highly turbid waters: application with SPOT data to quantify suspended particulate matter concentrations. *Remote Sens. Environ.* **81**, 149–161 (2002).
27. Koponen, S., Pulliainen, J., Kallio, K. & Hallikainen, M. Lake water quality classification with airborne hyperspectral spectrometer and simulated MERIS data. *Remote Sens. Environ.* **79**, 51–59 (2002).
28. Liu, J. P. et al. Sedimentary features of the Yangtze River-derived along-shelf clinoform deposit in the East China Sea. *Cont. Shelf Res.* **26**, 2141–2156 (2006).
29. Sterckx, S., Knaeps, E., Bollen, M., Trouw, K. & Houthuys, R. Retrieval of suspended sediment from advanced hyperspectral sensor data in the Scheldt estuary at different stages in the tidal cycle. *Mar. Geod.* **30**, 97–108 (2007).
30. Oyama, Y., Matsushita, B., Fukushima, T., Matsushige, K. & Imai, A. Application of spectral decomposition algorithm for mapping water quality in a turbid lake (Lake Kasumigaura, Japan) from Landsat TM data. *ISPRS J. Photogramm. Remote Sens.* **64**, 73–85 (2009).
31. Tarrant, P., Amacher, J. & Neuer, S. Assessing the potential of Medium-Resolution Imaging Spectrometer (MERIS) and Moderate-Resolution Imaging Spectroradiometer (MODIS) data for monitoring total suspended matter in small and intermediate sized lakes and reservoirs. *Wat. Resour. Res.* **46**, W09532 (2010).
32. Nechad, B., Ruddick, K. & Park, Y. Calibration and validation of a generic multisensor algorithm for mapping of total suspended matter in turbid waters. *Remote Sens. Environ.* **114**, 854–866 (2010).
33. Chen, S., Huang, W., Chen, W. & Chen, X. An enhanced MODIS remote sensing model for detecting rainfall effects on sediment plume in the coastal waters of Apalachicola Bay. *Mar. Environ. Res.* **72**, 265–272 (2011).
34. Knaeps, E., Dogliotti, A. I., Raymaekers, D., Ruddick, K. & Sterckx, S. In situ evidence of non-zero reflectance in the OLCI 1020 nm band for a turbid estuary. *Remote Sens. Environ.* **120**, 133–144 (2012).
35. Long, C. M. & Pavelsky, T. M. Remote sensing of suspended sediment concentration and hydrologic connectivity in a complex wetland environment. *Remote Sens. Environ.* **129**, 197–209 (2013).
36. Giardino, C., Bresciani, M., Stroppiana, D., Oggioni, A. & Morabito, G. Optical remote sensing of lakes: an overview on Lake Maggiore. *J. Limnol.* **73**, 201–214 (2014).
37. Feng, L., Hu, C., Chen, X. & Song, Q. Influence of the Three Gorges Dam on total suspended matters in the Yangtze Estuary and its adjacent coastal waters: Observations from MODIS. *Remote Sens. Environ.* **140**, 779–788 (2014).
38. Dorji, P. & Fearns, P. A quantitative comparison of total suspended sediment algorithms: a case study of the last decade for MODIS and Landsat-based sensors. *Remote Sens.* **8**, 810 (2016).
39. Dogliotti, A. I., Ruddick, K., Nechad, B., Doxaran, D. & Knaeps, E. A single algorithm to retrieve turbidity from remotely-sensed data in all coastal and estuarine waters. *Remote Sens. Environ.* **156**, 157–168 (2015).
40. Han, B. et al. Development of a semi-analytical algorithm for the retrieval of suspended particulate matter from remote sensing over clear to very turbid waters. *Remote Sens.* **8**, 211 (2016).
41. Yu, X. et al. An empirical algorithm to seamlessly retrieve the concentration of suspended particulate matter from water color across ocean to turbid river mouths. *Remote Sens. Environ.* **235**, 111491 (2019).
42. Zhang, X. On the estimation of biomass of submerged vegetation using Landsat thematic mapper (TM) imagery: a case study of the Honghu Lake, PR China. *Int. J. Remote Sens.* **19**, 11–20 (1998).
43. Vahtmäe, E., Kutser, T., Martin, G. & Kotta, J. Feasibility of hyperspectral remote sensing for mapping benthic macroalgal cover in turbid coastal waters—a Baltic Sea case study. *Remote Sens. Environ.* **101**, 342–351 (2006).
44. Dogan, O. K., Akyurek, Z. & Beklioglu, M. Identification and mapping of submerged plants in a shallow lake using quickbird satellite data. *J. Environ. Manage.* **90**, 2138–2143 (2009).
45. Yuan, L. & Zhang, L.-Q. Mapping large-scale distribution of submerged aquatic vegetation coverage using remote sensing. *Ecol. Inform.* **3**, 245–251 (2008).
46. Yadav, S. et al. A satellite-based assessment of the distribution and biomass of submerged aquatic vegetation in the optically shallow basin of Lake Biwa. *Remote Sens.* **9**, 966 (2017).
47. Pu, R., Bell, S., Baggett, L., Meyer, C. & Zhao, Y. Discrimination of seagrass species and cover classes with in situ hyperspectral data. *J. Coast. Res.* **28**, 1330–1344 (2012).
48. Visser, F., Wallis, C. & Sinnott, A. M. Optical remote sensing of submerged aquatic vegetation: opportunities for shallow clearwater streams. *Limnologica* **43**, 388–398 (2013).
49. Watanabe, F. S. Y., Imai, N. N., Alcântara, E. H., da Silva Rotta, L. H. & Utsumi, A. G. Signal classification of submerged aquatic vegetation based on the hemispherical–conical reflectance factor spectrum shape in the yellow and red regions. *Remote Sens.* **5**, 1856–1874 (2013).
50. Giardino, C. et al. Airborne hyperspectral data to assess suspended particulate matter and aquatic vegetation in a shallow and turbid lake. *Remote Sens. Environ.* **157**, 48–57 (2015).
51. Oyama, Y., Matsushita, B. & Fukushima, T. Distinguishing surface cyanobacterial blooms and aquatic macrophytes using Landsat/TM and ETM+ shortwave infrared bands. *Remote Sens. Environ.* **157**, 35–47 (2015).
52. Santos, M. J., Anderson, L. W. & Ustin, S. L. Effects of invasive species on plant communities: an example using submersed aquatic plants at the regional scale. *Biol. Invasions* **13**, 443–457 (2011).
53. Luo, J. et al. Applying remote sensing techniques to monitoring seasonal and interannual changes of aquatic vegetation in Taihu Lake, China. *Ecol. Indic.* **60**, 503–513 (2016).
54. Hou, X., Feng, L., Chen, X. & Zhang, Y. Dynamics of the wetland vegetation in large lakes of the Yangtze Plain in response to both fertilizer consumption and climatic changes. *ISPRS J. Photogramm. Remote Sens.* **141**, 148–160 (2018).
55. Brooks, C. N., Grimm, A. G., Marcarelli, A. M. & Dobson, R. J. Multiscale collection and analysis of submerged aquatic vegetation spectral profiles for Eurasian watermilfoil detection. *J. Appl. Remote Sens.* **13**, 037501 (2019).
56. Fritz, C., Kuhwald, K., Schneider, T., Geist, J. & Oppelt, N. Sentinel-2 for mapping the spatio-temporal development of submerged aquatic vegetation at Lake Starnberg (Germany). *J. Limnol.* **78**, 71–91 (2019).
57. Ghirardi, N. et al. Spatiotemporal dynamics of submerged aquatic vegetation in a deep lake from Sentinel-2 data. *Water* **11**, 563 (2019).
58. Niroumand-Jadidi, M., Pahlevan, N. & Vitti, A. Mapping substrate types and compositions in shallow streams. *Remote Sens.* **11**, 262 (2019).
59. Wilson, K. L., Skinner, M. A. & Lotze, H. K. Eelgrass (*Zostera marina*) and benthic habitat mapping in Atlantic Canada using high-resolution SPOT 6/7 satellite imagery. *Estuar. Coast. Shelf Sci.* **226**, 106292 (2019).
60. Niemeier, P. E. & Hubert, W. A. The 85-year history of the aquatic macrophyte species composition in a eutrophic prairie lake (United States). *Aquat. Bot.* **25**, 83–89 (1986).
61. Toshner, S. & Region-Brule, N. *Fishery Survey–Middle Eau Claire Lake Bayfield County, 2004–2005*. Report WBIC 2742100 (2006).
62. Depew, D. C., Houben, A. J., Ozersky, T., Hecky, R. E. & Guildford, S. J. Submerged aquatic vegetation in Cook's Bay, Lake Simcoe: assessment of changes in response to increased water transparency. *J. Great Lakes Res.* **37**, 72–82 (2011).
63. Vicencio, E. J. M. & Buot, I. E., Jr. Aquatic weed flora on the Southwest Lakeside of Laguna De Bay. *J Wetl Biodivers* **7**, 75–90 (2017).
64. Bond, W. & Roberts, M. The colonization of Cabora Bassa, Moçambique, a new man-made lake, by floating aquatic macrophytes. *Hydrobiologia* **60**, 243–259 (1978).
65. Istvánovics, V., Honti, M., Kovács, Á. & Osztoics, A. Distribution of submerged macrophytes along environmental gradients in large, shallow Lake Balaton (Hungary). *Aquat. Bot.* **88**, 317–330 (2008).
66. French, J. R. P. III Effect of submersed aquatic macrophytes on resource partitioning in yearling rock bass (Ambloplites rupestris) and pumpkinseeds (Lepomis gibbosus) in Lake St. Clair. *J. Great Lakes Res.* **14**, 291–300 (1988).
67. Balesic, H. Comparative ecology of four species of darters (Etheostominae) in Lake Dauphin and its tributary, the Valley River. MSc thesis, Univ. of Manitoba (1971).
68. Li, R., Zhang, Q.-Z., Jiang, Y.-B., Zhang, L. & Shao, X.-M. Species diversity of plant communities of Xingkai Lake wetlands under different levels of disturbance. *Wetland Science* **9**, 179–184 (2011).
69. Liu, W., Deng, W., Wang, G., Li, A. & Zhou, J. Aquatic macrophyte status and variation characteristics in the past 50 years in Hongzehu Lake. *J. Hydroecol* **2**, 1–8 (2009).
70. Shengzhao, Z. Aquatic vegetation in Hongze Lake. *J. Lake Sci.* **1**, 63–70 (1992).
71. Ward, J. & Talbot, J. Distribution of aquatic macrophytes in Lake Alexandrina, New Zealand. *N. Z. J. Mar. Freshw. Res.* **18**, 211–220 (1984).
72. Wang, S. & Dou, H. *Chinese Lake Catalogues* (Science Press, 1998).
73. Havens, K. E., Fox, D., Gornak, S. & Hanlon, C. Aquatic vegetation and largemouth bass population responses to water-level variations in Lake Okeechobee, Florida (USA). *Hydrobiologia* **539**, 225–237 (2005).
74. García, M. et al. Heavy metals in aquatic plants and their relationship to concentrations in surface water, groundwater and sediments-A case study of Poopó basin, Bolivia. *Rev. Boliv. Quím.* **22**, 11–18 (2005).
75. Fang, C. et al. Remote sensing of harmful algal blooms variability for Lake Hulun using adjusted FAI (AFAI) algorithm. *J. Environ. Inform.* **34**, 108–122 (2018).
76. Chen, Y. Studies on the potamogetonaceae in Qinghai Lake. *Acta Hydrobiol. Sin.* **11**, 228–235 (1987).
77. Pen, M. Vegetation types and distributions around Gyaring Lake and Ngoring Lake. *Acta Biol. Plateau Sin.* **7**, 71–79 (1987).
78. Li, W. Study on aquatic vegetation in Wulungu Lake, Xinjiang. *Oceanol. Limnol. Sin.* **24**, 100–108 (1993).
79. Machena, C. Zonation of submerged macrophyte vegetation in Lake Kariba, Zimbabwe and its ecological interpretation. *Vegetatio* **73**, 111–119 (1988).
80. Aladin, N., Filippov, A., Plotnikov, I., Orlova, M. & Williams, W. Changes in the structure and function of biological communities in the Aral Sea, with particular reference to the northern part (Small Aral Sea), 1985–1994: a review. *Int. J. Salt Lake Res.* **7**, 301–343 (1998).
81. Gabriel, A. O. & Bodensteiner, L. R. Impacts of riprap on wetland shorelines, upper Winnebago pool lakes, Wisconsin. *Wetlands* **32**, 105–117 (2012).
82. Badzinski, S. S., Ankney, C. D. & Petrie, S. A. in *Limnology and Aquatic Birds* 195–211 (Springer, 2006).
83. Chepinoga, V. V., Bergmeier, E., Rosbakh, S. A. & Fleckenstein, K. M. Classification of aquatic vegetation (Potametea) in Baikal Siberia, Russia, and its diversity in a northern Eurasian context. *Phytocoenologia* **43**, 127–167 (2013).
84. Jaikumar, M., Chellaiyan, D., Kanagu, L., Kumar, P. S. & Stella, C. Distribution and succession of aquatic macrophytes in Chilka Lake-India. *J. Ecol. Nat. Environ.* **3**, 499–508 (2011).
85. Krivonogov, S. K. et al. Regional to local environmental changes in southern Western Siberia: evidence from biotic records of mid to late Holocene sediments of Lake Beloye. *Palaeogeogr. Palaeoclimatol. Palaeoecol.* **331–332**, 177–193 (2012).
86. Romanova, S. & Kazangapova, N. *Theory and Practice of Selfpurification Capacities of Natural Water in Kazakhstan*. Technical Report (National Academy of Sciences of the Republic of Kazakhstan, 2018).

87. Villamagna, A. M., Murphy, B. R. & Karpanty, S. M. Community-level waterbird responses to water hyacinth (*Eichhornia crassipes*). *Invasive Plant Sci. Manag.* **5**, 353–362 (2012).
88. Imentai, A., Thevs, N., Schmidt, S., Nurtazin, S. & Salmurzauli, R. Vegetation, fauna, and biodiversity of the Ile delta and southern Lake Balkhash—a review. *J. Great Lakes Res.* **41**, 688–696 (2015).
89. Barrientos, C. A. *Fish Abundance and Community Composition in Native and Non-Native Littoral Aquatic Plants at Lake Izabal, Guatemala*. MSc thesis, Univ. of Florida (2005).
90. Tehranchi, M., Shafiei, A. D. & Shaghaghi, S. Studying solutions of development of tourism in Urmia Lake based on SWOT model. *Adv. Environ. Biol.* **2013**, 4505–4512 (2013).
91. Davies, W. D. Lake Nicaragua fishery resources in *Investigations of the ichthyofauna of Nicaraguan Lakes* (ed. Thorson, T. B.) 16 (Univ. of Nebraska Lincoln, 1976).
92. Cheruiyot, E. et al. Evaluating MERIS-based aquatic vegetation mapping in Lake Victoria. *Remote Sens.* **6**, 7762–7782 (2014).
93. Heblinski, J. et al. High-resolution satellite remote sensing of littoral vegetation of Lake Sevan (Armenia) as a basis for monitoring and assessment. *Hydrobiologia* **661**, 97–111 (2011).
94. Beklioglu, M., Altinayar, G. & Tan, C. O. Water level control over submerged macrophyte development in five shallow lakes of Mediterranean Turkey. *Arch. Hydrobiol.* **166**, 535–556 (2006).
95. Green, J. in *The Nile* (ed. Dumont H. J.) 263–286 (Springer, 2009).
96. Kalman, L. S. & Peltzer, G. R. Simulation of Landsat Thematic Mapper imagery using AVIRIS hyperspectral imagery. In *4th Annual JPL Airborne Geoscience Workshop* (1993).

Acknowledgements This work was supported by the Strategic Priority Research Program of Chinese Academy of Sciences (XDA20060402), the National Natural Science Foundation of China (numbers 41971304, 41890852 and 41890851) and by High-level Special Funding of the Southern University of Science and Technology (numbers G02296302, G02296402). We thank Guangzhou Water Color Ocean Technology Co., Ltd and Easy Ocean Technology Ltd for their help in collecting in situ data.

Author contributions L.F. initiated the project and wrote an initial draft of the manuscript, and Y.D., X.H. and Y.X. performed the data processing and analysis. All authors participated in interpreting the results and revising the manuscript.

Competing interests The authors declare no competing interests.

Additional information

Supplementary information The online version contains supplementary material available at https://doi.org/10.1038/s41586-021-03254-3.

Correspondence and requests for materials should be addressed to L.F.

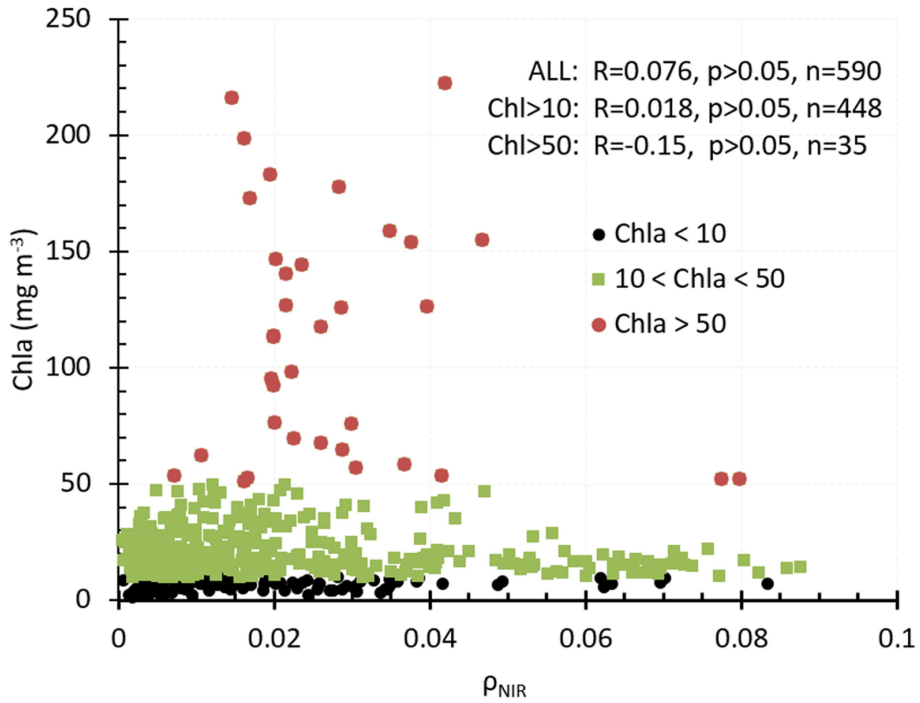

Extended Data Fig. 1 | Relationship between the surface reflectance in the NIR band (ρ_{NIR}) and Chl*a*. The correlations for different Chl*a* ranges (colour-coded) and individual lakes are non-significant ($P > 0.05$). The data are from in situ measurements collected from 15 lakes in China across waters with varying eutrophic status. ρ_{NIR} values are the equivalent L5TM NIR reflectances aggregated using in situ hyperspectral measurements and the L5TM spectral response function (see the aggregation method in Kalmen et al.[96]).

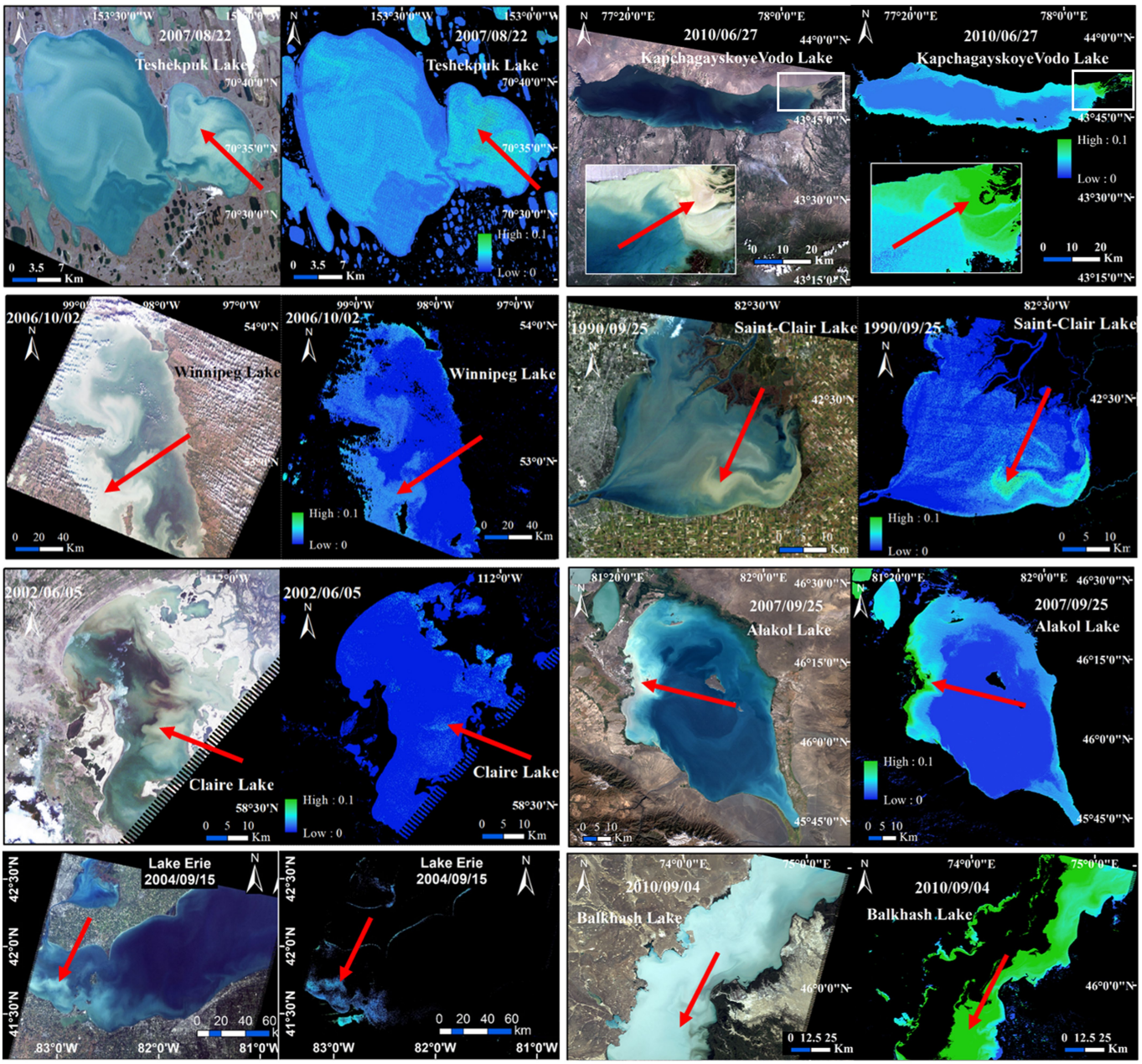

Extended Data Fig. 2 | Examples showing the effects of high sediment loads on the bloom intensity (B_{NIR}) calculations in eight of the lakes studied in Ho et al.[1]. The left panels of the paired images show the true-colour composites for L5TM images, and the right panels show the corresponding B_{NIR} maps after applying the hue and Fmask masks. The sediment plumes (indicated by red arrows) with high B_{NIR} values (~0.1) could still be classified as intense blooms with the hue mask defined in Ho et al.[1]. The examination of historical L5TM images show that sediment plumes could occur in at least 58 (82%) of the 71 lakes studied in Ho et al.[1].

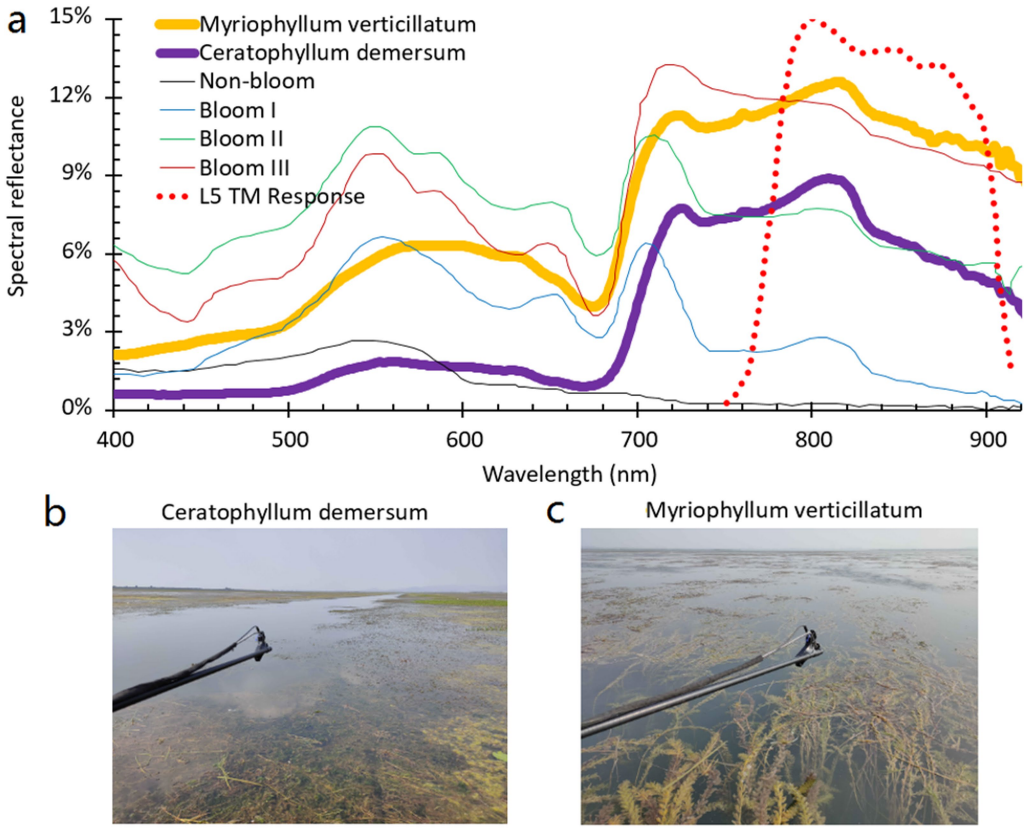

Extended Data Fig. 3 | Reflectance spectra of submerged vegetation. **a**, The spectral reflectances of two types (*Ceratophyllum demersum* and *Myriophyllum verticillatum*) of submerged vegetation collected from Taihu Lake in China (a shallow lake ~200 km away from Hongze Lake) on 24 October 2019, using the PSR+3500 field-portable spectrometer manufactured by Spectral Evolution. Also plotted are the spectral reflectances of different blooms and the normalized spectral responses in the L5TM NIR band, which were obtained from extended data figure 7 in Ho et al.[1]. The spectral features of submerged vegetation, particularly the reflectance in the NIR band, are very similar to those of intense phytoplankton blooms. **b**, **c**, Photographs taken while conducting the in situ measurements.

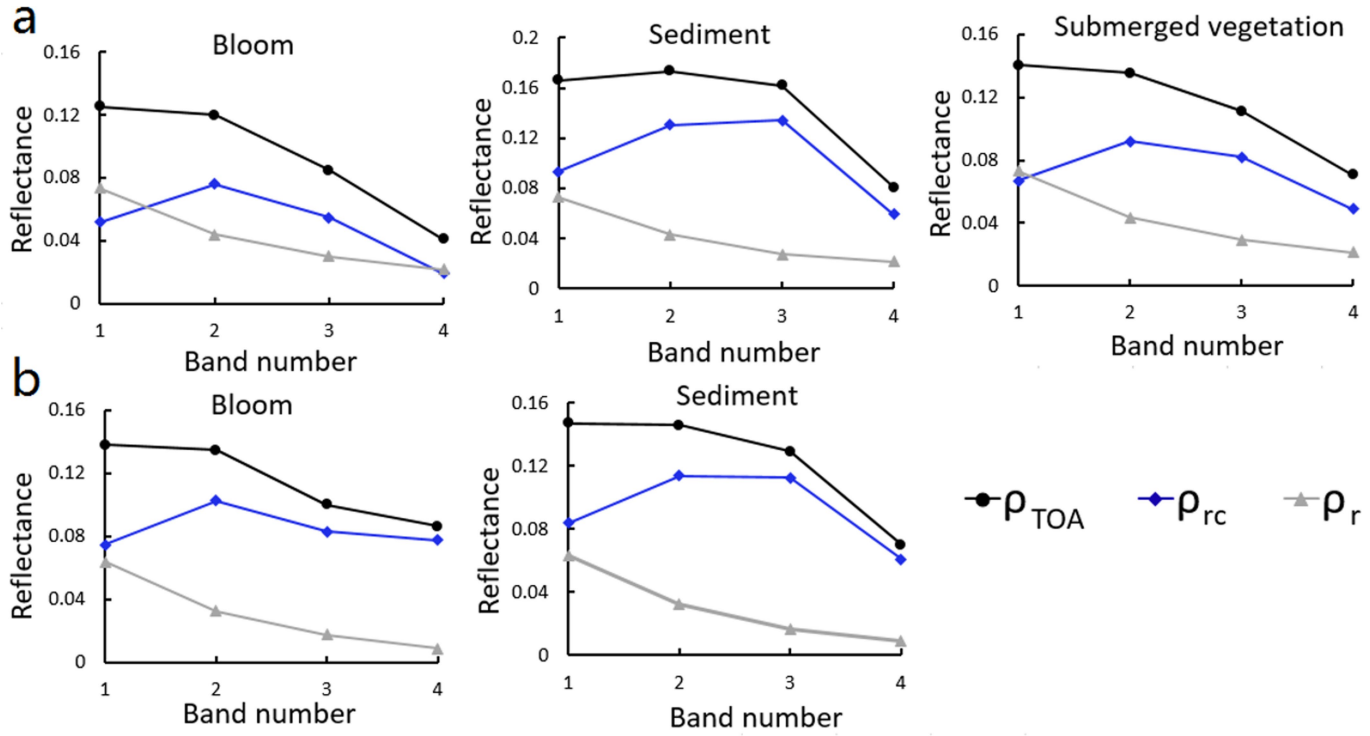

Extended Data Fig. 4 | Spectral features of different types of waters in L5TM images. a, **b**, The spectral data were obtained from the arrow-indicated pixels in Fig. 1 (**a** from Songkhla Lake and **b** from Hongze Lake). ρ_{TOA} is the top-of-atmosphere reflectance, ρ_r is the reflectance from molecular scattering (or Rayleigh scattering, estimated using the method in Gordon[10]) and ρ_{rc} is the difference between ρ_{TOA} and ρ_r.

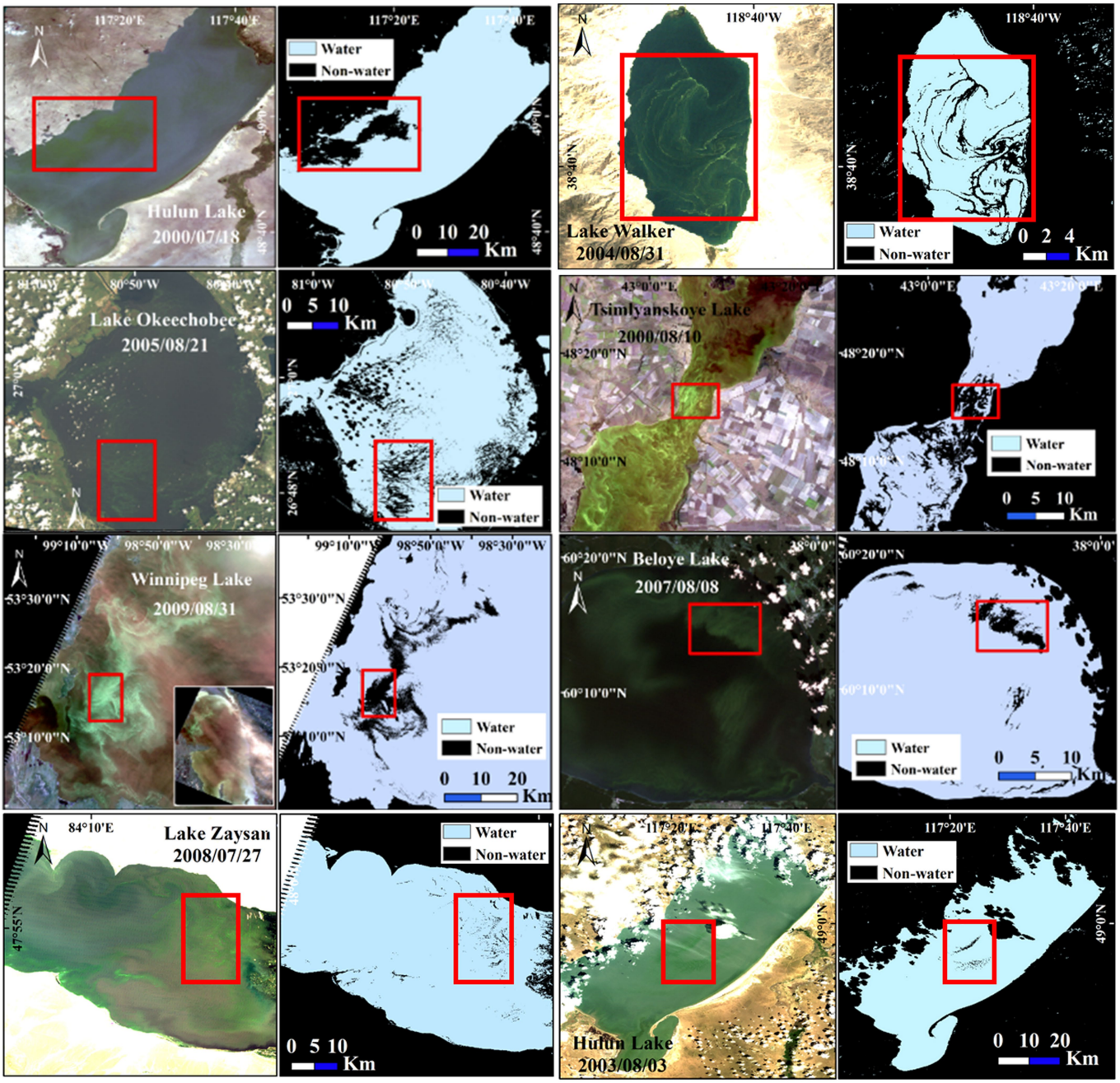

Extended Data Fig. 5 | Examples of pixels with intense blooms erroneously masked by Fmask in eight of the lakes studied in Ho et al.[1]. The left panels of the paired images show the true-colour composites for the L5TM images, and the right panels show the resultant separation of pixels determined using Fmask. Clearly, intense blooms (greenish in the red squares) have been classified as other classes instead of as water. The examination of the lakes studied in ref. [1] showed that most of the severe blooms with surface scum were missed owing to the improper use of Fmask.

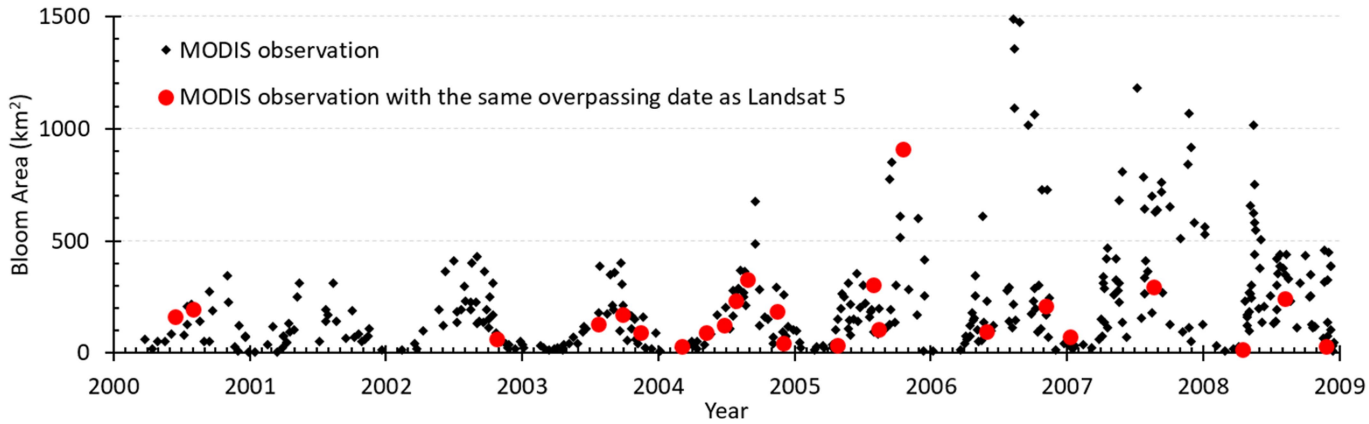

Extended Data Fig. 6 | Daily areas of algal bloom in Taihu Lake between 2000 and 2008, determined using MODIS observations by Hu et al.[12]**.** Red points represent MODIS observations with the same overpassing dates as L5TM (that is, daily MODIS observations have concurrent L5TM images) and indicate the difficulty in characterizing long-term bloom dynamics. For example, whereas black dots show a clear increase in bloom area after 2005, such a trend is difficult to capture with the red dots.

Extended Data Table 1 | Previous studies with in situ datasets that showed substantial effects of water turbidity (or total suspended sediments, TSS) on the reflectance of the water column in the NIR band

References	Location(s)	Range of turbidity (NTU) /TSS (mg/L)
Büttner et al. [16]	**Balaton Lake, Hungary**	**69.0-591.0 mg/L**
Bukata et al. [17]	**Saint-Clair Lake, Canada and United States**	**2.5-20.0 mg/L**
Nas et al. [18]	**Beysehir Lake, Turkey**	**0.1-15.5 mg/L**
Binding et al. [19]	**Lake Erie, United States**	**0.18-28.26 mg/L**
Matthews et al. [20]	**Zeekoevlei Lake, South Africa**	**0.03-50 mg/L**
Wang et al. [7]	**Lake Okeechobee, United States**	**1-300 NTU**
Kaba et al. [21]	**Tana Lake, Ethiopia**	**~0-240.0 mg/L**
Hamed [22]	**Nasser Lake, Egypt**	**0.75-78.4 NTU**
Zeng & Binding [23]	**Winnipeg Lake, Canada, and Lake Erie, Canada and United States**	**0.01-31.6 mg/L**
Mikkelsen [24]	Four coastal regions, Denmark and Ebro River, Spain	0.5-24.6 mg/L
Dekker et al. [25]	Frisian lakes, Netherlands	1.6-255.0 mg/L
Doxaran et al [26]	Gironde Estuary, France	35-2072 mg/L
Koponen et al [27]	Four lakes in Finland	0-30 NTU
Liu et al. [28]	Middle Yangtze River, China	23.4–61.2 mg/L
Sterckx et al. [29]	Scheldt River, Belgium	13-336 mg/L
Oyama et al. [30]	Lake Kasumigaura, Japan	17.6-47.9 mg/L
Tarrant et al. [31]	Roosevelt and Bartlett Pleasant Lake, United States	0.30–13.4 mg/L
Nechad et al. [32]	Southern North Sea, Europe	1.24-110.27 mg/L
Chen et al. [33]	Apalachicola Bay, United States	1.29–208 mg/L
Knaeps et al. [34]	Scheldt, Belgium and the Netherlands	15-402 mg/L
Long & Pavelsky [35]	Peace–Athabasca Delta, Canada	0-4000 mg/L
Giardino et al. [36]	Lake Maggiore, Italy	0.5-100 mg/L
Feng et al. [37]	Yangtze Estuary, China	4.3-1762.1 mg/L
Dorji & Fearns [38]	Simulated datasets	0.01-7000.0 mg/L
Dogliotti et al. [39]	Southern North Sea; Guyana coastal waters, Scheldt, Gironde, France; and Río de la Plata estuary, South America	1.8-988 mg/L
Han et al. [40]	European coastal waters; French Guiana; Eastern Vietnam Sea; China Yellow Sea; and northern Canada	0.15-2626.0 mg/L
Yu et al. [41]	Gulf of Mexico and Massachusetts Bay, United States; Yangtze Estuary, China; European coastal waters; the Río de La Plata Estuary, South America	0.2-2068.8 mg/L

The bold text indicates studies of lakes that were also included in Ho et al.[1]. We note that this table does not include all related studies, because a complete list would be too long to present here. Data from refs. [7,16–41].

Extended Data Table 2 | Previous studies with in situ datasets that showed that NIR reflectance could be substantially enhanced owing to the presence of submerged vegetation

References	Location(s)	Major vegetation species
Zhang et al. [42]	Honghu Lake, China	*Potamogeton maackianus* Benn., *Myriophyllum spicatum, Hydrilla verticillata* Royle, *Ceratophyllum oryzetorum* Kom. *and Potamogeton lucens* Linn.
Vahtmäe et al. [43]	Baltic Sea, Europe	*Cladophora glomerata, Furcellaria lumbricalis, and Fucus vesiculosus*
Dogan et al. [44]	Lake Mogan,Turkey	*Potamogeton pectinatus, Najas sp and Myriophyllum spicatum*
Yuan & Zhang [45]	Chongming Island, China	*Myriophyllum spicatum*
Yadav et al. [46]	Lake Biwa, Japan	Unknown
Pu et al. [47]	Florida coast, United States	*Syringodium filiforme, Thalassia testudinum,and Halodule wrightii.*
Visser et al. [48]	River Wylye and River Frome, UK	*Myriophyllum spicatum, Ranunculus fluitans and Potamogeton pectinatus*
Watanabe et al. [49]	Ferreira stream, Brazil	*Ceratophyllum demersum*
Giardino et al. [50]	Lake Trasimeno, Italy	*Potamogeton pectinatusand Myriophyllum spicatum*
Oyama et al. [51]	Lakes Kasumigaura, Inba-numa and Tega-numa, Japan	*Trapa natans*
Santos et al. [52]	Sacramento San Joaquin River Delta, United States	*Myriophyllum spicatum and Egeria densa*
Luo et al. [53]	Lake Taihu, China	*Vallisneria spiralis, Ceratophyllum demersum, Potamogeton malaianus, P. maackianus,* and *Hydrilla verticillata*
Hou et al. [54]	25 lakes, China	Unknown
Brooks et al. [55]	Lake Huron, United States	*M. spicatum and Myriophyllum sibiricum*
Fritz et al. [56]	Lake Starnberg, Germany	*Chara spp.and Potamogeton spp.*
Ghirardi et al. [57]	Lake Iseo, Italy	*Vallisneria spiralis and Najas marina*
Niroumand-Jadidi [58]	Sarca River, Italy	Unknown
Wilson et al. [59]	Atlantic coast of Nova Scotia, Canada	*Zostera marina*

This table does not include all related studies, because a complete list would be too long to present here. Data from refs. [42–59].

Extended Data Table 3 | List of lakes studied in Ho et al.[1] with abundant submerged vegetation identified

ID	Lake name	Country	References
1	Clear	United States	Niemeier and Hubert [60]
2	Claire	Canada	Toshner and Region-Brule [61]
3	Simcoe	Canada	Depew et al. [62]
4	Bay	Philippines	Vicencio and Buot Jr [63]
5	CaboraBassa	Mozambique Zimbabwe	Bond and Roberts [64]
6	Balaton	Hungary	Istvánovics et al. [65]
7	Saint-Clair	Canada United States	French III [66]
8	Dauphin	Canada	Balesic [67]
9	Khanka	Russia China	Li et al. [68]
10	Hongze	China	Liu et al. [69]; Shengzhao [70]
11	Alexandrina	Australia	Ward and Talbot [71]
12	Bosten	China	Wang and Dou [72]
13	Okeechobee	United States	Havens et al. [73]
14	Poopo	Bolivia	García et al. [74]
15	Hulun	China	Fang et al. [75]
16	Songkhla	Thailand	Sompongchaiyakul et al. [9]
17	Qinghai	China	Chen [76]
18	Gyaring	China	Pen [77]
19	Ulungar	China	Li [78]
20	Ngoring	China	Pen [77]
21	Se-lin	China	Wang and Dou [72]
22	Kariba	Zimbabwe Zambia	Machena [79]
23	Aral-Sea	Kazakhstan Uzbekistan	Aladin et al. [80]
24	Winnebago	United States	Gabriel and Bodensteiner [81]
25	Erie	Canada United States	Badzinski et al. [82]
26	Baikal	Russia	Chepinoga et al. [83]
27	Chilka	India	Jaikumar et al. [84]
28	Cha-jihNan-mu-tso--Zhari-Namco	China	Wang and Dou [72]
29	Beloye	Russia	Krivonogov et al. [85]
30	Sasykkol	Kazakhstan	Romanova and Kazangapova [86]
31	Chapala	Mexico	Villamagna et al. [87]
32	Balkhash	Kazakhstan	Imentai et al. [88]
33	Izabal	Guatemala	Barrientos [89]
34	Urmia	Iran	Tehranchi et al. [90]
35	Nicaragua	Nicaragua	Davies [91]
36	Alakol	Kazakhstan	Romanova and Kazangapova [86]
37	Victoria	Tanzania Uganda Kenya	Cheruiyot et al. [92]
38	Sevan	Armenia	Heblinski et al. [93]
39	Beysehir	Turkey	Beklioglu et al. [94]
40	Nasser	Egypt Sudan	Green [95]
41	Edward	Zaire Uganda	Green [95]

Data from refs. [9,60–95].

nature research

Corresponding author(s): Lian Feng

Last updated by author(s): Nov 6, 2020

Reporting Summary

Nature Research wishes to improve the reproducibility of the work that we publish. This form provides structure for consistency and transparency in reporting. For further information on Nature Research policies, see our Editorial Policies and the Editorial Policy Checklist.

Statistics

For all statistical analyses, confirm that the following items are present in the figure legend, table legend, main text, or Methods section.

n/a	Confirmed	
☐	☒	The exact sample size (*n*) for each experimental group/condition, given as a discrete number and unit of measurement
☐	☒	A statement on whether measurements were taken from distinct samples or whether the same sample was measured repeatedly
☐	☒	The statistical test(s) used AND whether they are one- or two-sided *Only common tests should be described solely by name; describe more complex techniques in the Methods section.*
☒	☐	A description of all covariates tested
☒	☐	A description of any assumptions or corrections, such as tests of normality and adjustment for multiple comparisons
☐	☒	A full description of the statistical parameters including central tendency (e.g. means) or other basic estimates (e.g. regression coefficient) AND variation (e.g. standard deviation) or associated estimates of uncertainty (e.g. confidence intervals)
☐	☒	For null hypothesis testing, the test statistic (e.g. *F*, *t*, *r*) with confidence intervals, effect sizes, degrees of freedom and *P* value noted *Give P values as exact values whenever suitable.*
☒	☐	For Bayesian analysis, information on the choice of priors and Markov chain Monte Carlo settings
☐	☒	For hierarchical and complex designs, identification of the appropriate level for tests and full reporting of outcomes
☐	☒	Estimates of effect sizes (e.g. Cohen's *d*, Pearson's *r*), indicating how they were calculated

Our web collection on statistics for biologists contains articles on many of the points above.

Software and code

Policy information about availability of computer code

Data collection	The satellite data were obtained from the U.S. Geological Survey at https://glovis.usg.gov. The in situ spectral and Chla data were collected by authors.
Data analysis	ArcGIS (version 10.8) and ENVI (version 5.4) were used to analyze the satellite images

For manuscripts utilizing custom algorithms or software that are central to the research but not yet described in published literature, software must be made available to editors and reviewers. We strongly encourage code deposition in a community repository (e.g. GitHub). See the Nature Research guidelines for submitting code & software for further information.

Data

Policy information about availability of data

All manuscripts must include a data availability statement. This statement should provide the following information, where applicable:

- Accession codes, unique identifiers, or web links for publicly available datasets
- A list of figures that have associated raw data
- A description of any restrictions on data availability

The Landsat data can be obtained from the U.S. Geological Survey at https://glovis.usg.gov. The in situ spectral and Chla data are available from the Supporting Information

Field-specific reporting

Please select the one below that is the best fit for your research. If you are not sure, read the appropriate sections before making your selection.

☐ Life sciences ☐ Behavioural & social sciences ☒ Ecological, evolutionary & environmental sciences

For a reference copy of the document with all sections, see nature.com/documents/nr-reporting-summary-flat.pdf

Ecological, evolutionary & environmental sciences study design

All studies must disclose on these points even when the disclosure is negative.

Study description	This study questioned the veracity of the phytoplankton bloom trends in global lakes derived from Landsat measurements by Ho et al., 2019.
Research sample	Two separate samples were selected. 1) in situ data were used to demonstrate the the use of NIR reflectance as a proxy for algae bloom strength is questionable, and 2) satellite images were used to show the erroneous bloom detections using the method presented by Ho et al. 2019.
Sampling strategy	The Landsat data used in our study were from the same lakes that were studied by Ho et al. 2019, and acquisition dates for the data were also fall within their studied summertime.
Data collection	Cruise surveyed in situ data were collected by the authors in 15 large lakes on the Yangtze Plain of China.
Timing and spatial scale	In situ data from 15 lakes in China were collected across four different seasons between 2005 and 2019, and Landsat data covers several lakes that were studied by Ho et al. 2019.
Data exclusions	No data were excluded from analysis.
Reproducibility	Our results could easily be reproduced with existing datasets.
Randomization	The Landsat data were randomly selected from USGS, while only images with small cloud cover were used. All the in situ spectral and Chla data from our filed surveys were used in the study.
Blinding	Not applicable in our study.

Did the study involve field work? ☐ Yes ☐ No

Field work, collection and transport

Field conditions	No precipitation and strong wind occurred when sampling.
Location	15 Lakes on the Yangtze Plain of China, Lat: 29°-30°N, Lon: 112°-122°E
Access & import/export	Not applicable in our study.
Disturbance	NASA-recommended ocean optics protocol (Mobley 1999) was followed when conducting reflectance measurements, to minimize the uncertainties from reflection at the air-water interface.

Reporting for specific materials, systems and methods

We require information from authors about some types of materials, experimental systems and methods used in many studies. Here, indicate whether each material, system or method listed is relevant to your study. If you are not sure if a list item applies to your research, read the appropriate section before selecting a response.

Materials & experimental systems

n/a	Involved in the study
☒	☐ Antibodies
☒	☐ Eukaryotic cell lines
☒	☐ Palaeontology and archaeology
☒	☐ Animals and other organisms
☒	☐ Human research participants
☒	☐ Clinical data
☒	☐ Dual use research of concern

Methods

n/a	Involved in the study
☒	☐ ChIP-seq
☒	☐ Flow cytometry
☒	☐ MRI-based neuroimaging

Reply to: Concerns about phytoplankton bloom trends in global lakes

https://doi.org/10.1038/s41586-021-03255-2

Published online: 17 February 2021

Check for updates

Jeff C. Ho[1,2]✉, Anna M. Michalak[1]✉ & Nima Pahlevan[3,4]

REPLYING TO L. Feng et al. *Nature* https://doi.org/10.1038/s41586-021-03254-3 (2021)

In Ho et al.[1], we used three decades of high-resolution Landsat 5 (L5TM) satellite imagery to investigate long-term trends in intense summertime near-surface phytoplankton blooms for 71 large lakes globally to reveal a global exacerbation of bloom conditions. In the accompanying Comment[2], Feng et al. question whether the implemented algorithm is "a reliable proxy for bloom strength" owing to the strong effects of suspended sediments and aquatic vegetation, and whether "the infrequent satellite observations from L5TM make it difficult to draw statistically meaningful conclusions". We agree that these are important considerations, and they have been examined in detail. In Ho et al.[3], the algorithm was found to outperform ten other candidate algorithms (see table 1 in ref. [3]). The 11 algorithms were evaluated using a total of ten metrics that assessed the algorithms' ability to capture bloom magnitude, interannual variability and seasonal variability when evaluated against both in situ biovolume observations[4] and remote-sensing imagery from MERIS and MODIS[5]. In Ho et al.[1], we further evaluated the algorithm by assessing its ability to reproduce previously reported spatial gradients across 48 region pairs in 22 lakes (see section 'Validation of well known spatial gradients in bloom intensity' and supplementary table 2 in ref. [1]). In addition, to evaluate whether trends in the abundance of constituents such as suspended sediments or aquatic vegetation could be misinterpreted as trends in bloom intensity, we assessed the algorithm's ability to capture both the direction and the timing of changes in bloom intensity for seven lakes for which such information was available in the literature (see section 'Evaluation of bloom intensity time series and trends' in ref. [1]). In all analyses, the algorithm was shown to meaningfully and accurately represent long-term trends in bloom intensity for lakes for which such information was available. Although we recognize that modern remote-sensing instruments[6] will be able to track lacustrine algal blooms even more accurately in the future, we maintain that the analysis presented in Ho et al.[1] using L5TM represents the best possible analysis of global phytoplankton bloom intensity over the historical period going back to the 1980s.

In elaborating on the above two topics, Feng et al.[2] present measurements of near-infrared (NIR) reflectance versus chlorophyll *a* co-mingled across 15 unidentified lakes in China (see extended data figure 1 in ref. [2]), whereas in Ho et al.[1] we explicitly state that while the approach implemented therein "has proven effective in identifying the extent of near-surface intense phytoplankton blooms, we emphasize that the retrieval of concentrations of specific bloom severity metrics (for example, chlorophyll *a*) is beyond the scope of this study". In Ho et al.[1] we also explain that the implemented approach was designed specifically to eliminate the need to compare absolute magnitudes across lakes—a barrier that has limited cross-lake syntheses in the past. For these two reasons, the data presented by Feng et al.[2] are not directly relevant to the arguments presented in Ho et al.[1].

Feng et al.[2] then elaborate that "the effect of water turbidity on B_{NIR} should be evaluated carefully". We agree, and this was indeed done in Ho et al.[1,3]. As stated above, the algorithm was validated across over two dozen lakes, including an extensive discussion of suspended sediments in Ho et al.[3]. In figure 1 of ref. [2] (and extended data figures 2, 4), Feng et al. use true-colour composite examples from lakes in Ho et al.[1] to argue that sediments can be a confounding factor for the efficacy of the algorithm from Ho et al.[1]. However, the simple occurrence of sediment plumes does not imply that long-term trends based on the algorithm are incorrect. Indeed, several of the lakes included in extended data table 1 of Feng et al.[2] (for example, Lakes Balaton, Winnipeg and Erie) were included in the algorithm evaluation in Ho et al.[1] (see figure 4a and extended data figures 9a, 9c in ref. [1]), and their multi-decadal bloom intensity trends were successfully reproduced by the algorithm. Furthermore, visual interpretation of true-colour imagery alone can be misleading as a method for the delineation of blooms, sediment and submerged vegetation. Indeed, past studies that compared inferences from qualitative observations and remote sensing yielded ambiguous results[7], which is part of a broader challenge in relating in situ and remote-sensing observations[8].

Feng et al.[2] then argue that "the growth of aquatic vegetation can lead to overestimation of bloom severity". Overall, in optically deep waters in the NIR region, it is very unlikely that the water-leaving signal carries any information pertaining to submerged vegetation, owing to strong absorption by pure water[9]. The key question, however, is not whether submerged vegetation could in some cases affect NIR reflectance (extended data table 2 and extended data figure 3 in ref. [2]) or whether some of the examined lakes have submerged vegetation (extended data table 3 in ref. [2]), but rather whether trends in the abundance of submerged vegetation could affect the reported trends in bloom intensity. As described above, the algorithm was successfully validated in lakes with well documented trends in bloom intensity, including some of those with submerged vegetation listed in extended data table 3 of ref. [2]. More broadly, we did not find that the observed trends in bloom intensity tracked documented trends in submerged vegetation for lakes for which such information is available. For example, Havens et al.[10] (see figure 5 therein) report the annual spatial extent of submerged aquatic vegetation for Lake Okeechobee for 2002–2015. The trends in submerged vegetation do not track the observed historical trend in bloom intensity in Ho et al.[1] (see figure 4f therein). There is therefore no indication that trends in submerged aquatic vegetation influenced estimates of long-term trends in bloom intensity.

Feng et al.[2] then raise concerns about the hue mask. We again refer to the above summary of how the algorithm was validated across over two dozen lakes, including the discussion about suspended sediments and turbidity. We agree that surface reflectance data could be used

[1]Department of Global Ecology, Carnegie Institution for Science, Stanford, CA, USA. [2]Department of Civil & Environmental Engineering, Stanford University, Stanford, CA, USA. [3]NASA Goddard Space Flight Center, Greenbelt, MD, USA. [4]Science Systems and Applications Inc., Lanham, MD, USA. ✉e-mail: jeffho@alumni.stanford.edu; michalak@carnegiescience.edu

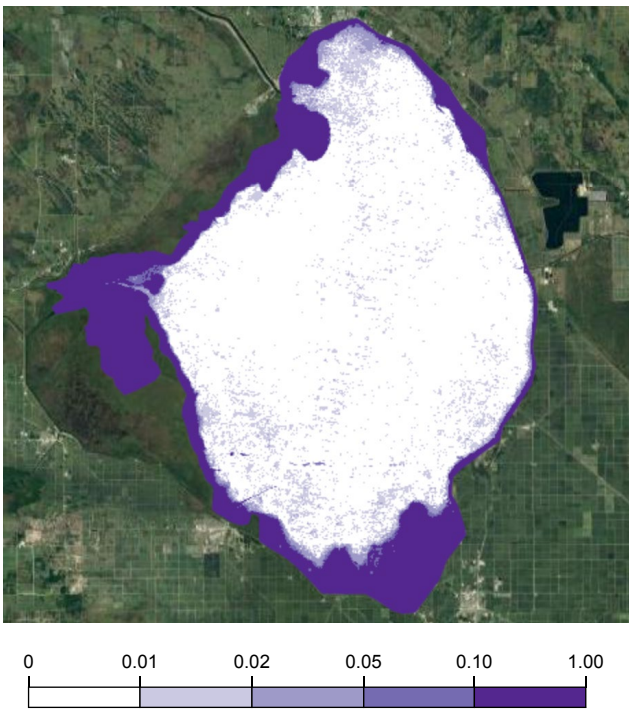

Fig. 1 | Detections of 'land' from Fmask over open water are rare. The map shows the fraction of detections of 'land' from Fmask over Lake Okeechobee from 1984 to 2012 for the months of June to October (242 image composites). Image values are only valid within the Lake polygon boundary. Basemap data from Google[15], TerraMetrics Inc. (www.terrametrics.com).

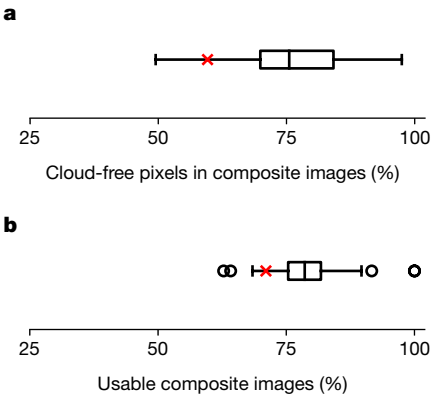

Fig. 2 | The average cloud-free area is large in the L5TM images used in Ho et al.[1] study lakes, and the percentage of usable images is therefore also high. a, For each 16-day composite image created for each lake in Ho et al.[1], the cloud-free percentage of the image was calculated as one minus the number of cloud pixels divided by the number of image pixels. Then, for each lake, the cloud-free percentages were averaged across all images to yield an average cloud-free percentage for each lake, presented as a boxplot across the 71 studied lakes. The mean and median across the lakes are 77% and 76% cloud-free pixels, respectively. **b**, For each lake, the percentage of usable composite images was determined by removing individual images with less than 80% cloud-free pixels, or less than the mean observed surface area minus one standard deviation[1]. The percentage of usable images is presented as a boxplot across the 71 studied lakes. The mean and median across lakes are both 79% of the composites retained. The red symbols indicate the respective values for Taihu Lake, which was not among the 71 studied lakes. In the boxplots, the boxes indicate the interquartile range (IQR) and the whiskers denote the largest value <1.5×IQR above the third quartile and the smallest value >1.5×IQR below the first quartile. The circles indicate outliers beyond the whisker values.

in future work to further refine the analysis, but such data were not available at the time of the analysis and are not expected to alter the fundamental conclusions of the work.

Next, Feng et al.[2] comment on the use of the Fmask algorithm for cloud clearing and for identifying water pixels. Extended data figure 5 of ref. [2] shows examples of cases where the bloom intensity may be so high as to lead the Fmask algorithm to erroneously identify portions of open water as land. Again taking Lake Okeechobee (shown in extended data figure 5 of ref. [2]) as an example, we examined every scene over the period of record used in Ho et al.[1] and identified the frequency with which pixels in open water were erroneously identified as land using the Fmask algorithm. We confirmed that this can indeed happen in isolated cases, but this is a rare occurrence. Figure 1 shows the fraction of cases, across the 242 scene composites obtained between 1984 and 2012 for the months of June to October, for which a given 30-m pixel within the lake is identified as land. For the open-water portions of the lake, this fraction is below 3%. This illustrates that the Fmask algorithm performs as designed, with variability in the lake boundary and in the near-shore regions being filtered out, whereas the open water where bloom activity occurs is included in almost all composites. Finally, because in Ho et al.[1] we normalize the bloom time series for each lake, the focus is on long-term relative trends in bloom severity, rather than on pixel-by-pixel classification for a particular scene.

Finally, Feng et al.[2] raise the issue of frequency of observations and cloud cover, and state that because "the global mean daily cloud-free probability is 33%", only one-third of L5TM overpasses are usable. Setting aside the issue that sun glint, one of the "unfavourable observational conditions" resulting in unusable images, as claimed in ref. [2], is not possible with L5TM data owing to viewing angles below 7.5°, the percentage quoted by Feng et al.[2] is in no way representative of the data availability for ref. [1]. On average, 75% of the area in the L5TM images over the studied lakes over the study period was cloud-free (Fig. 2a). The vast underestimate of cloud-free area in Feng et al.[2] is likely due to the fact that it is based on global cloud cover, which includes high cloud cover over oceans[11], does not account for greater cloud cover seasonality over land[11] and is calculated from a cloud cover algorithm designed specifically to designate more pixels as cloud versus clear sky in order to be conservative[12].

Extended data figure 6 in ref. [2] also presents MODIS data for Taihu Lake[13] (a lake not included in Ho et al.[1]) for cloud-free days based on an earlier study[13], and identify those days with coincident L5TM overpasses to argue that L5TM observations are too sparse to track trends. In Ho et al.[1], we selected lakes on the basis of their inclusion in previous studies that leveraged remote sensing by satellites[14], thus reducing the likelihood that persistent cloudiness obscured the images. Furthermore, we used the Fmask algorithm (https://code.earthengine.google.com/dataset/LANDSAT/LT5_L1T_TOA_FMASK) to objectively identify cloud and cloud shadow pixels (Fig. 2a), whereas the study[13] referenced in extended data figure 6 of ref. [2] subjectively "visually examined" images and reported that only images "with minimal cloud cover were chosen and processed"[13]. Also, unlike ref. [13], we did not exclude all composites with any cloud cover, but only those in which the observed lake surface area was less than 80% of the maximum, or less than the mean minus one standard deviation of the whole surface area of the lake for the time series, whichever was lower. Overall, we were able to use an average of 79% of L5TM images for the lakes included in the study (Fig. 2b). If Lake Taihu had been included in the study, we would have retained 71% of the L5TM images over the study period for that lake (Fig. 2b), or an average of 6.4 images per June–October period, rather than the average 1.4 images per June–October period implied by the red symbols in extended data figure 6 of ref. [2].

Overall, although we appreciate the careful analysis presented in Feng et al.[2], none of the issues presented therein had any substantive impact on the analysis and conclusions in Ho et al.[1]. Specifically, we saw no evidence that the presence of suspended sediments or aquatic

vegetation affected the long-term trends estimated for the examined lakes, and cloud cover did not reduce data availability to a degree that affected the ability to estimate long-term trends.

Reporting summary

Further information on research design is available in the Nature Research Reporting Summary linked to this paper.

Data availability

Data availability is as outlined in ref. [1].

1. Ho, J. C., Michalak, A. M. & Pahlevan, N. Widespread global increase in intense lake phytoplankton blooms since the 1980s. *Nature* **574**, 667–670 (2019).
2. Feng, L. et al. Concerns about phytoplankton bloom trends in global lakes. *Nature* https://doi.org/10.1038/s41586-021-03254-3 (2021).
3. Ho, J. C., Stumpf, R. P., Bridgeman, T. B. & Michalak, A. M. Using Landsat to extend the historical record of lacustrine phytoplankton blooms: a Lake Erie case study. *Remote Sens. Environ.* **191**, 273–285 (2017).
4. Bridgeman, T. B., Chaffin, J. D. & Filbrun, J. E. A novel method for tracking western Lake Erie *Microcystis* blooms, 2002–2011. *J. Great Lakes Res.* **39**, 83–89 (2013).
5. Wynne, T. T. & Stumpf, R. P. Spatial and temporal patterns in the seasonal distribution of toxic cyanobacteria in Western Lake Erie from 2002–2014. *Toxins* **7**, 1649–1663 (2015).
6. Mishra, S. et al. Measurement of cyanobacterial bloom magnitude using satellite remote sensing. *Sci. Rep.* **9**, 18310 (2019).
7. Ho, J. C. & Michalak, A. M. Challenges in tracking harmful algal blooms: a synthesis of evidence from Lake Erie. *J. Great Lakes Res.* **41**, 317–325 (2015).
8. Bertani, I. et al. Tracking cyanobacteria blooms: do different monitoring approaches tell the same story? *Sci. Total Environ.* **575**, 294–308 (2017).
9. Mobley, C. D. *Light and Water: Radiative Transfer in Natural Waters* (Academic Press, 1994).
10. Havens, K. et al. Extreme weather events and climate variability provide a lens to how shallow lakes may respond to climate change. *Water* **8**, 229 (2016).
11. King, M. D., Platnick, S., Menzel, W. P., Ackerman, S. A. & Hubanks, P. A. Spatial and temporal distribution of clouds observed by MODIS onboard the Terra and Aqua satellites. *IEEE Trans. Geosci. Remote Sens.* **51**, 3826–3852 (2013).
12. Ackerman, S. A. et al. Discriminating clear sky from clouds with MODIS. *J. Geophys. Res.* **103**, 32141–32157 (1998).
13. Hu, C. et al. Moderate Resolution Imaging Spectroradiometer (MODIS) observations of cyanobacteria blooms in Taihu Lake, China. *J. Geophys. Res.* **115**, C04002 (2010).
14. Sharma, S. et al. A global database of lake surface temperatures collected by in situ and satellite methods from 1985–2009. *Sci. Data* **2**, 150008 (2015).
15. Gorelick, N. et al. Google Earth Engine: planetary-scale geospatial analysis for everyone. *Remote Sens. Environ.* **202**, 18–27 (2017).

Author contributions J.C.H. and A.M.M. designed the research and analysed the results. J.C.H. and A.M.M. wrote the response with input from N.P. J.C.H. performed the majority of the computations with input from A.M.M.

Competing interests The authors declare no competing interests.

Additional information
Supplementary information The online version contains supplementary material available at https://doi.org/10.1038/s41586-021-03255-2.
Correspondence and requests for materials should be addressed to J.C.H. or A.M.M.
Reprints and permissions information is available at http://www.nature.com/reprints.
Publisher's note Springer Nature remains neutral with regard to jurisdictional claims in published maps and institutional affiliations.

nature research

Corresponding author(s): *Double-blind peer review submissions: write DBPR and your manuscript number here instead of author names.*

Last updated by author(s): *YYYY-MM-DD*

Reporting Summary

Nature Research wishes to improve the reproducibility of the work that we publish. This form provides structure for consistency and transparency in reporting. For further information on Nature Research policies, see our Editorial Policies and the Editorial Policy Checklist.

Statistics

For all statistical analyses, confirm that the following items are present in the figure legend, table legend, main text, or Methods section.

n/a	Confirmed	
☐	☒	The exact sample size (*n*) for each experimental group/condition, given as a discrete number and unit of measurement
☐	☒	A statement on whether measurements were taken from distinct samples or whether the same sample was measured repeatedly
☒	☐	The statistical test(s) used AND whether they are one- or two-sided *Only common tests should be described solely by name; describe more complex techniques in the Methods section.*
☒	☐	A description of all covariates tested
☒	☐	A description of any assumptions or corrections, such as tests of normality and adjustment for multiple comparisons
☐	☒	A full description of the statistical parameters including central tendency (e.g. means) or other basic estimates (e.g. regression coefficient) AND variation (e.g. standard deviation) or associated estimates of uncertainty (e.g. confidence intervals)
☒	☐	For null hypothesis testing, the test statistic (e.g. *F*, *t*, *r*) with confidence intervals, effect sizes, degrees of freedom and *P* value noted *Give P values as exact values whenever suitable.*
☒	☐	For Bayesian analysis, information on the choice of priors and Markov chain Monte Carlo settings
☒	☐	For hierarchical and complex designs, identification of the appropriate level for tests and full reporting of outcomes
☒	☐	Estimates of effect sizes (e.g. Cohen's *d*, Pearson's *r*), indicating how they were calculated

Our web collection on statistics for biologists contains articles on many of the points above.

Software and code

Policy information about availability of computer code

Data collection	Google Earth Engine's web interface allows the FMask cloud detection algorithm to be applied on any Landsat 5 Thematic Mapper images. Access will be provided upon request.
Data analysis	*Provide a description of all commercial, open source and custom code used to analyse the data in this study, specifying the version used OR state that no software was used.*

For manuscripts utilizing custom algorithms or software that are central to the research but not yet described in published literature, software must be made available to editors and reviewers. We strongly encourage code deposition in a community repository (e.g. GitHub). See the Nature Research guidelines for submitting code & software for further information.

Data

Policy information about availability of data

All manuscripts must include a data availability statement. This statement should provide the following information, where applicable:

- Accession codes, unique identifiers, or web links for publicly available datasets
- A list of figures that have associated raw data
- A description of any restrictions on data availability

The Landsat 5 Thematic Mapper imagery used in this study is available from the US Geological Survey (http://earthexplorer.usgs.gov) and through Google Earth Engine (https://earthengine.google.com).

Field-specific reporting

Please select the one below that is the best fit for your research. If you are not sure, read the appropriate sections before making your selection.

☐ Life sciences ☐ Behavioural & social sciences ☒ Ecological, evolutionary & environmental sciences

For a reference copy of the document with all sections, see nature.com/documents/nr-reporting-summary-flat.pdf

Ecological, evolutionary & environmental sciences study design

All studies must disclose on these points even when the disclosure is negative.

Study description	This study used historical satellite imagery, and the other questions below therefore do not apply.
Research sample	*Describe the research sample (e.g. a group of tagged Passer domesticus, all Stenocereus thurberi within Organ Pipe Cactus National Monument), and provide a rationale for the sample choice. When relevant, describe the organism taxa, source, sex, age range and any manipulations. State what population the sample is meant to represent when applicable. For studies involving existing datasets, describe the data and its source.*
Sampling strategy	*Note the sampling procedure. Describe the statistical methods that were used to predetermine sample size OR if no sample-size calculation was performed, describe how sample sizes were chosen and provide a rationale for why these sample sizes are sufficient.*
Data collection	*Describe the data collection procedure, including who recorded the data and how.*
Timing and spatial scale	*Indicate the start and stop dates of data collection, noting the frequency and periodicity of sampling and providing a rationale for these choices. If there is a gap between collection periods, state the dates for each sample cohort. Specify the spatial scale from which the data are taken*
Data exclusions	*If no data were excluded from the analyses, state so OR if data were excluded, describe the exclusions and the rationale behind them, indicating whether exclusion criteria were pre-established.*
Reproducibility	*Describe the measures taken to verify the reproducibility of experimental findings. For each experiment, note whether any attempts to repeat the experiment failed OR state that all attempts to repeat the experiment were successful.*
Randomization	*Describe how samples/organisms/participants were allocated into groups. If allocation was not random, describe how covariates were controlled. If this is not relevant to your study, explain why.*
Blinding	*Describe the extent of blinding used during data acquisition and analysis. If blinding was not possible, describe why OR explain why blinding was not relevant to your study.*

Did the study involve field work? ☐ Yes ☒ No

Reporting for specific materials, systems and methods

We require information from authors about some types of materials, experimental systems and methods used in many studies. Here, indicate whether each material, system or method listed is relevant to your study. If you are not sure if a list item applies to your research, read the appropriate section before selecting a response.

Materials & experimental systems

n/a	Involved in the study
☒	☐ Antibodies
☒	☐ Eukaryotic cell lines
☒	☐ Palaeontology and archaeology
☒	☐ Animals and other organisms
☒	☐ Human research participants
☒	☐ Clinical data
☒	☐ Dual use research of concern

Methods

n/a	Involved in the study
☒	☐ ChIP-seq
☒	☐ Flow cytometry
☒	☐ MRI-based neuroimaging